AJNR

Image-Quality Assessment of 3D Intracranial Vessel Wall MRI Using DANTE or DANTE-CAIPI for Blood Suppression and Imaging Acceleration

B. Sannananja, C. Zhu, C.G. Colip, A. Somasundaram, M. Ibrahim, T. Khrisat and M. Mossa-Basha

AJNR Am J Neuroradiol 2022, 43 (6) 837-843
doi: https://doi.org/10.3174/ajnr.A7531
http://www.ajnr.org/content/43/6/837

Image-Quality Assessment of 3D Intracranial Vessel Wall MRI Using DANTE or DANTE-CAIPI for Blood Suppression and Imaging Acceleration

B. Sannananja, C. Zhu, C.G. Colip, A. Somasundaram, M. Ibrahim, T. Khrisat, and M. Mossa-Basha

ABSTRACT

BACKGROUND AND PURPOSE: 3D intracranial vessel wall MRI techniques are time consuming and prone to artifacts, especially flow artifacts. Our aim was to compare the image quality of accelerated and flow-suppressed 3D intracranial vessel wall MR imaging techniques relative to conventional acquisitions.

MATERIALS AND METHODS: Consecutive patients undergoing MR imaging had conventional postcontrast 3D T1-sampling perfection with application-optimized contrasts by using different flip angle evolution (SPACE) and either postcontrast delay alternating with nutation for tailored excitation (DANTE) flow-suppressed or DANTE–controlled aliasing in parallel imaging results in higher acceleration (CAIPI) flow-suppressed and accelerated T1-SPACE sequences performed. The sequences were evaluated using 4- or 5-point Likert scales for overall image quality, SNR, extent/severity of artifacts, motion, blood suppression, sharpness, and lesion assessment. Quantitative assessment of lumen and wall-to-lumen contrast ratios was performed.

RESULTS: Eighty-nine patients were included. T1-DANTE-SPACE had significantly better qualitative ratings relative to T1-SPACE for image quality, SNR, artifact impact, arterial and venous suppression, and lesion assessment ($P < .001$ for each, respectively), with the exception of motion ($P = .16$). T1-DANTE-CAIPI-SPACE had significantly better image quality, lesion assessment, arterial and venous blood suppression, less artifact impact, and less motion compared with T1-SPACE ($P < .001$ for each, respectively). The SNR was higher with T1-SPACE compared with T1-DANTE-CAIPI-SPACE ($P < .001$). T1-DANTE-CAIPI-SPACE showed significantly worse lumen ($P = .005$) and wall-to-lumen contrast ratios ($P = .001$) compared with T1-SPACE, without a significant difference between T1-SPACE and T1-DANTE-SPACE. T1-DANTE-CAIPI-SPACE scan time was 5:11 minutes compared with 8:08 and 8:41 minutes for conventional T1-SPACE and T1-DANTE-SPACE, respectively.

CONCLUSIONS: Accelerated postcontrast T1-DANTE-CAIPI-SPACE had fewer image artifacts, less motion, improved blood suppression, and a shorter scan time, but lower qualitative and quantitative SNR ratings relative to conventional T1-SPACE intracranial vessel wall MR imaging. Postcontrast T1-DANTE-SPACE had superior SNR, blood suppression, higher image quality, and fewer image artifacts, but slightly longer scan times relative to T1-SPACE.

ABBREVIATIONS: CAIPI = controlled aliasing in parallel imaging results in higher acceleration; DANTE = delay alternating with nutation for tailored excitation; IVW = intracranial vessel wall MR imaging; MSDE = motion-sensitized driven-equilibrium; SPACE = sampling perfection with application-optimized contrasts by using different flip angle evolution

Intracranial vessel wall MR imaging (IVW) has shown value in vasculopathy differentiation and characterization;[1-6] however, there is substantial technique and imaging parameter heterogeneity.[3,6-14] There are a number of challenges that currently exist with IVW in terms of its application and implementation. One challenge is technique-related, specifically artifactual arterial and venous wall enhancement that can mimic pathology. Small studies have shown that artifactual enhancement on postcontrast conventional 3D variable refocusing flip angle T1-weighted techniques can mimic aneurysm wall enhancement.[10,15] Blood-suppression techniques can suppress such artifactual flow, including delay alternating with nutation for tailored excitation (DANTE) and motion-sensitized

Received December 27, 2021; accepted after revision April 13, 2022.

From the Department of Radiology (B.S., A.S.), Emory University, Atlanta, Georgia; Department of Radiology (C.Z., M.M.-B.), University of Washington, Seattle, Washington; Kaiser Permanente Northwest (C.G.C.), Portland, OR; Department of Radiology (M.I.), University of Kansas, Lawrence, Kansas; and Department of Surgery (T.K.), Lincoln Medical Center, New York, New York.

This work was supported by National Institutes of Health grants (NIH R01 NS092207-04, NIH R01 NS092207-04S1.

Please address correspondence to Mahmud Mossa-Basha, MD, University of Washington, Department of Radiology, 1959 NE Pacific St., Seattle, WA 98195; e-mail: mmossab@uw.edu; @mossabas

http://dx.doi.org/10.3174/ajnr.A7531

Table 1: Pulse sequence acquisition parameters

	3D T1-SPACE	DANTE-CAIPI-T1-SPACE	DANTE-T1-SPACE
TR/TE (ms)	1000/11.0	1000/11.0	1000/11.0
In-plane resolution (mm)	0.56 × 0.56	0.56 × 0.56	0.56 × 0.56
Section thickness (mm)	0.56	0.56	0.56
Flip angle	Variable	Variable	Variable
FOV (mm)	180 × 180	180 × 180	180 × 180
Parallel imaging factor	2	2	2
Averages	1	1	1
Scan time (min)	8:08	5:11	8:47
DANTE	No	Yes	Yes
CAIPI	No	Yes	No

driven equilibrium (MSDE).[7,16] MSDE has proved to be very valuable in carotid vessel wall MR imaging; however, this technique results in signal reduction and T2 signal decay,[17] which can limit its value for intracranial pathologies due to the need for high resolution for the evaluation of smaller, thinner-walled, tortuous intracranial arteries and smaller vascular pathologic lesions.[3]

Another challenge in IVW implementation is long scan times for conventional IVW sequences and protocols, which can add 16–20 minutes of scan time for pre- and postcontrast T1-weighted IVW sequences and much more for multicontrast protocols, which can be restrictive in clinical settings and also lead to increased motion artifacts. A number of acceleration techniques have been developed and used in IVW, including controlled aliasing in parallel imaging results in higher acceleration (CAIPI), which is a parallel imaging technique optimized for 3D acquisitions.[14,18,19]

To our knowledge, no prior study has compared conventional IVW with blood-suppressed or blood-suppressed and accelerated IVW in a real-world clinical cohort evaluating patients with diverse intracranial vasculopathies. In the current study, we performed quantitative and qualitative assessment of postcontrast T1-sampling perfection with application-optimized contrasts by using different flip angle evolution (SPACE; Siemens) IVW in comparison with either DANTE or DANTE-CAIPI T1-SPACE IVW, performed during the same scan as part of clinical IVW protocols, to determine which IVW technique may optimize image quality and reduce flow artifacts, while, in the case of CAIPI acquisitions, also reducing scan time.

MATERIALS AND METHODS

Patient Selection

This study was approved by the University of Washington institutional ethics committee, and informed consent was obtained from all study participants. Consecutive patients who underwent IVW examinations from January 2017 to April 2019 for suspected intracranial vascular disease were extracted from the institutional database. We collected demographic and clinical data: age, sex, and suspected initial and final clinical diagnoses.

Image Acquisition

All imaging was performed on a 3T Prisma MR imaging system (Siemens) using a 64-channel neurovascular coil. The imaging protocol included precontrast and postcontrast T1-SPACE. Each patient also underwent another postcontrast T1-weighted IVW sequence, either postcontrast T1WI DANTE-CAIPI-SPACE or postcontrast T1-DANTE-SPACE. The sequence of acquisition for postcontrast images was randomized with patients imaged with T1-SPACE followed by the other techniques and vice versa. The sequence scan parameters are listed in Table 1. Scan time was 8:08 for T1-SPACE, 5:11 for T1-DANTE-CAIPI-SPACE, and 8:41 for T1-DANTE-SPACE.

Image Evaluation

Two board-certified neuroradiologists (M.M.-B., with 16 years, and C.G.C., with 9 years of radiology experience, respectively), blinded to the patient clinical information, independently evaluated individual postcontrast IVW sequences. All imaging studies were de-identified, and the raters were unaware of the sequence acquisition during review. Each individual postcontrast sequence was reviewed in random order on a RadiAnt DICOM viewer (https://www.radiantviewer.com/) with 3-plane reconstructed views, in conjunction with review of the precontrast T1-weighted sequence and the TOF-MRA. Raters evaluated overall imaging quality on the following 4-point scale: 1, optimal image quality; 2, minimally limited; 3, limited but interpretable; and 4, nondiagnostic. Image SNR was evaluated on the following 4-point scale: 1, optimal SNR; 2, mildly diminished SNR not affecting image interpretation; 3, mildly-to-moderately diminished SNR limiting image interpretation; 4, markedly diminished SNR that renders the images uninterpretable. Image artifacts were evaluated on the following 5-point scale: 1, no artifacts; 2, trace artifacts; 3, artifacts not affecting the targeted arterial anatomy; 4, artifacts mildly affecting the targeted arterial anatomy; and 5, artifacts obscuring the targeted anatomy. Arterial blood suppression was evaluated on the following 4-point scale: 1, complete blood suppression; 2, minimal central luminal flow artifacts; 3, luminal flow artifacts mimicking lesions in 1–2 segments; 4, luminal flow artifacts mimicking lesions in >2 segments. Lesion assessment for arterial wall abnormalities were evaluated on the following 4-point scale: 1, well-visualized with sharp margins; 2, minimal blurring with loss of margins but pattern and structure of involvement clear; 3, structure of involvement clear but pattern of involvement limited; 4, lesion pattern and structure involved cannot be determined.

Cases interpretable for lesion pattern (1 or 2 ratings) for both acquisitions were reviewed for patterns (eccentric, <50% circumferential wall involvement, versus concentric, ≥50% circumferential wall involvement) on each acquisition (T1-SPACE and T1-DANTE-SPACE or T1-DANTE-CAIPI-SPACE). For cases with multiple lesions, the pattern for most stenotic lesions was recorded. Consensus was reached when there was disagreement on the pattern. Venous flow suppression was evaluated on the following 4-

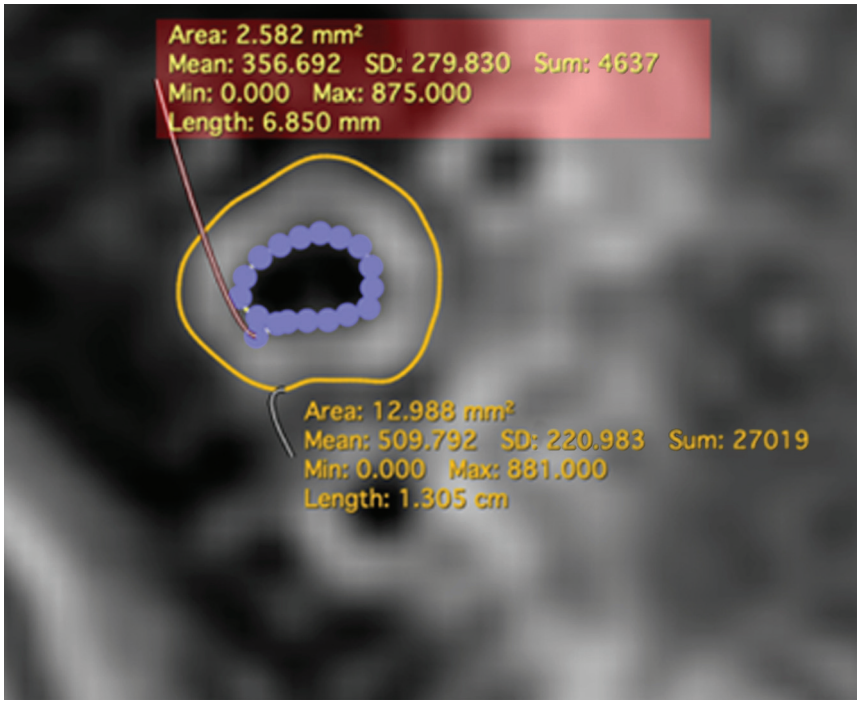

FIG 1. Quantitative measurement technique. Manual ROIs were drawn on representative images tracing the interface between the wall and lumen (luminal contour) and between the wall and surrounding tissues (outer wall contour). Total area of the vessel (area within the outer contour), luminal area (area within the inner contour), mean signal intensity, and SD were recorded for each patient. Sum indicates the sum of signal intensities within the selected region; Min, minimum; Max, maximum.

point scale: 1, no venous artifacts (complete suppression); 2, minimal central or peripheral nonsuppression that does not mimic a lesion; 3, central and peripheral nonsuppression that does not mimic a lesion; 4, flow nonsuppression that mimics pathology. Specific types of artifacts encountered on individual imaging acquisitions were recorded (motion, reduced SNR, arterial, and venous flow artifacts). Motion was graded on a 5-point Likert scale: 0, no motion; 1, minimal; 2, mild; 3, moderate; and 4, severe motion, based on a previously established scoring scale.[20] Arterial flow artifacts were documented for all acquisitions involving the following segments: vertebral arteries, petrous ICAs, cavernous ICAs, supraclinoid ICAs, M1 MCA, ≥M2 MCAs, P1 posterior cerebral artery, ≥P2 posterior cerebral arteries, A1 anterior cerebral artery, ≥A2 anterior cerebral arteries, and the basilar artery. Venous flow artifacts were recorded involving the following structures: dural venous sinsuses, cortical veins, and deep veins.

In addition to qualitative imaging evaluation, quantitative evaluation was performed by a separate board-certified neuroradiologist (B.S., with 5 years of radiology experience). For each patient, manual ROIs were drawn on representative images from each postcontrast T1-SPACE, T1-DANTE-CAIPI-SPACE, and T1-DANTE-SPACE sequence (Fig 1). Measurements were performed on both diseased and normal segments, with ROI placement selected randomly between the posterior and anterior circulation for the normal-segment assessment. For those being assessed for intracranial vasculopathy (intracranial atherosclerotic disease, vasculitis, and so forth.), the measurement was taken from the lesion, while for those undergoing IVW for aneurysm postcoiling, normal segments were selected. Two contours were generated tracing the interface between the wall and lumen (luminal contour) and between the wall and surrounding tissues (outer wall contour) using a freehand drawing tool (Horos, Lesser General Public License, Version 3.3.6; https://horosproject.org). The total area of the vessel (area within the outer contour), lumen area (area within the inner contour), mean signal intensity, and SD were recorded. Additional ROIs measuring 3 mm^2 in diameter were drawn in the normal-appearing cortical gray matter, in close proximity to the vessel being quantitatively analyzed for comparison. All measurements, labeling, and areas analyzed were saved for future reference and reproducibility assessment. Wall area was calculated as the difference in the total area of the vessel subtracted from the lumen area. The lumen contrast ratio was calculated using the following formula: Average Lumen Signal on a Single Section/Average Gray Matter Signal. The wall-to-lumen contrast ratio was determined using the following formula: Average Wall Signal on a Single Section/Average Lumen Signal. For quantitative measurement-reproducibility assessment, 30 randomly selected cases were analyzed using the same methodology and location by a second reviewer (A.S., with 2 years of radiology experience).

Statistical Analysis

Analysis was performed using SPSS, Version 23.0 (IBM). Because not all the data were normally distributed as evaluated by the Kolmogorov-Smirnov test, all the data were expressed as median and interquartile range. The Wilcoxon matched-pairs signed-rank test was used to compare the measurements between different techniques. Rater values were averaged for the various sequence comparisons. A paired Student *t* test was used to compare the performance of the 2 sequences. The interobserver agreement was evaluated with the intraclass correlation coefficient, with absolute agreement and a 2-way random model. $P < .05$ was regarded as significant, and all *P* values were 2-sided.

RESULTS

Patient Data

A total of 96 subjects were reviewed; however, 7 early studies were excluded because T1-CAIPI-SPACE was performed without DANTE blood suppression. A total of 89 patients were included in the final analysis (55 women [61.8%]; 22–80 years of age; median age, 53 years). Of these 89 patients, 64 patients were imaged with postcontrast T1-DANTE-CAIPI-SPACE, and 25, with T1-DANTE-SPACE. The most common final clinical diagnoses were intracranial atherosclerotic disease in 33 patients and postaneurysm

Table 2: Patient demographics

Characteristics	Cohort
Age (age group) (median)	22–80 years, median age, 53 years
Sex (%)	
Male	34 (38.2%)
Female	55 (61.8%)
Clinical indication for IVW MR imaging	
Intracranial atherosclerotic disease	33
Aneurysm postcoiling/Pipeline stent/clipping	31
Vasculitis	11
Moyamoya disease/syndrome	3
Aneurysm	4
CADASIL	2
Radiation vasculopathy	1
Cryptogenic stroke	4

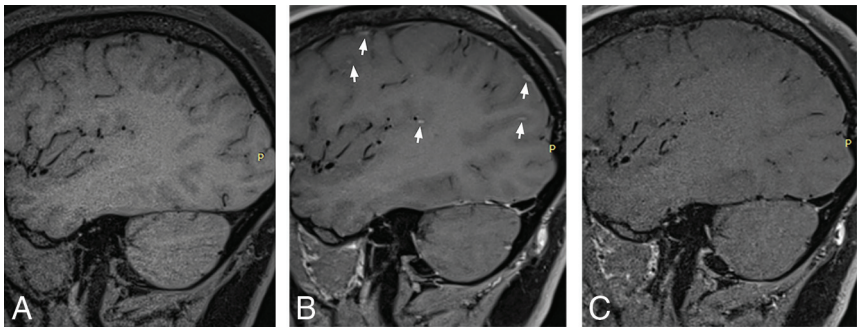

FIG 2. When we compare sagittal TI-SPACE precontrast (*A*) and sagittal TI-SPACE postcontrast (*B*), there are multiple focal enhancing lesions seen along the cortical surface (*small arrows*) on postcontrast IVW. On TI-DANTE-CAIPI-SPACE (*C*), the cortically based enhancing lesions disappear. The enhancing foci represent nonsuppression of blood signal in small cortical veins.

treatment in 31 patients. Complete patient demographic and diagnosis information is shown in Table 2.

Qualitative Assessment

T1-DANTE-CAIPI-SPACE was rated higher than T1-SPACE for overall image quality (2, 1.5–2.5, versus 2.5, 2–3; $P < .001$). T1-DANTE-CAIPI-SPACE had significantly lower SNR (2, 2–2.5, versus 1.5, 1–2, $P < .001$), better arterial-suppression ratings (1.25, 1–1.5, versus 3, 2.5–3.5; $P < .001$) (Online Supplemental Data), better artifact ratings (3, 2–3, versus 3.5, 3–4, $P < .001$) (Online Supplemental Data), better venous blood suppression (1.5, 1.125–2 versus 3, 2–3.375; $P < .001$) (Fig 2), and better lesion-assessment ratings (1.5, 1–2, versus 2, 1.5-2.5; $P < .001$) compared with T1-SPACE (Online Supplemental Data). Forty-seven (73%) T1-SPACE series were adequate for lesion-pattern assessment (1 or 2); 54 (84%), on T1-DANTE-CAIPI-SPACE; and 43 (67%) were adequate on both. See Table 3 for complete T1-SPACE and T1-DANTE-CAIPI-SPACE comparison.

T1-DANTE-SPACE had significantly higher overall image quality (2, 1.5-2.5, versus 2.5, 2–3; $P < .001$), higher SNR (2, 1.5–2.5, versus 2, 2–2.5; $P < .001$), better artifact ratings (2.5, 2–3, versus 3.5, 3–4; $P < .001$), and improved arterial (1.5, 1–1.875, versus 3, 2.625–3.5; $P < .001$) (Fig 3) and venous (2, 1.5–2, versus 3, 2–3; $P < .001$) blood suppression (Fig 3) and lesion-assessment ratings (1.75, 1–2, versus 2.5, 2–3; $P < .001$). Fourteen (56%) cases were adequate for lesion-pattern assessment on T1-SPACE, 22 (88%), on T1-DANTE-SPACE, and 14 (56%), on both. See Table 4 for complete T1-SPACE and T1-DANTE-SPACE comparison.

Artifact Comparison

There was a significant difference in motion impact and scoring between T1-SPACE and T1-DANTE-CAIPI-SPACE (0, 0–0.5, versus 1, 0–2; $P < .001$) (Table 3 and Online Supplemental Data). T1-SPACE and T1-DANTE-CAIPI-SPACE showed moderate or severe motion on 25% and 6.3% of comparative acquisitions, respectively. There was no significant difference in motion between T1-SPACE and T1-DANTE-SPACE ($P = .5$) (Table 4 and Online Supplemental Data). T1-SPACE and T1-DANTE-SPACE each showed moderate or severe motion on 48% of comparative acquisitions.

For T1-SPACE acquisitions, the arterial segments most frequently affected by arterial flow artifacts were the V3/V4 vertebral artery segments (75.3%) (Online Supplemental Data), the petrous ICA (44.9%), M2 MCA (10.1%), and P2 of the posterior cerebral artery (4.5%). Venous flow artifacts were most frequently encountered on T1-SPACE involving the cortical veins (65.2%), dural venous sinuses (36%), and deep veins (13.5%). See the Online Supplemental Data for full details on artifacts encountered.

Quantitative Assessment

Quantitative comparisons are listed in Tables 3 and 4. There was no significant difference between T1-SPACE and T1-DANTE-CAIPI-SPACE for lumen area or wall area comparisons. The lumen contrast ratio was significantly higher with T1-DANTE-CAIPI-SPACE (0.37, 0.27–0.48, versus 0.33, 0.26–0.43; $P = .003$), possibly due to increased background noise affecting lumen measures or alterations in gray matter values; and wall-to-lumen contrast ratio was significantly lower (1.9, 1.7–2.5, versus 2.3, 1.9–2.6; $P < .001$), indicating a worse wall-to-lumen signal, likely from increased background noise. There were no significant differences in the lumen area, wall area, lumen contrast ratio, or wall-to-lumen contrast ratio for the T1-SPACE and T1-DANTE-SPACE comparison.

Agreement Analysis

Interreader agreement scores for the qualitative and quantitative assessments are listed in the Online Supplemental Data. Interreader agreement for lesion assessment (0.745) was moderate. The remaining qualitative image parameters, including image quality, SNR, artifact severity, motion, and arterial and venous blood suppression, had good-to-excellent agreement (0.771–0.938). The highest

Table 3: SPACE versus DANTE-CAIPI-SPACE (average score of 2 reviewers)[a]

	SPACE	DANTE-CAIPI-SPACE	*P* Value
Qualitative measurements			
Image quality	2.5 (2–3)	2 (1.5–2.5)	<.001
SNR	1.5 (1–2)	2 (2–2.5)	<.001
Artifacts	3.5 (3–4)	3 (2–3)	<.001
Art. blood suppression	3 (2.5–3.5)	1.25 (1–1.5)	<.001
Lesion	2 (1.5–2.5)	1.5 (1–2)	<.001
Ven. blood suppression	3 (2–3.375)	1.5 (1.125–2)	<.001
Motion	1 (0–2)	0 (0–0.5)	<.001
Quantitative measurement			
Lumen area (mm^2)	7.9 (5.5–10.3)	7.6 (4.8–11.0)	.45
Wall area (mm^2)	12.6 (9.9–16.3)	12.4 (10.1–14.6)	.04
Lumen CR	0.33 (0.26–0.43)	0.37 (0.27–0.48)	.003
Wall lumen CR	2.3 (1.9–2.6)	1.9 (1.7–2.5)	<.001

Note:—Art. indicates arterial; Ven., venous; CR, contrast ratio.
[a] Values are expressed as median (interquartile range).

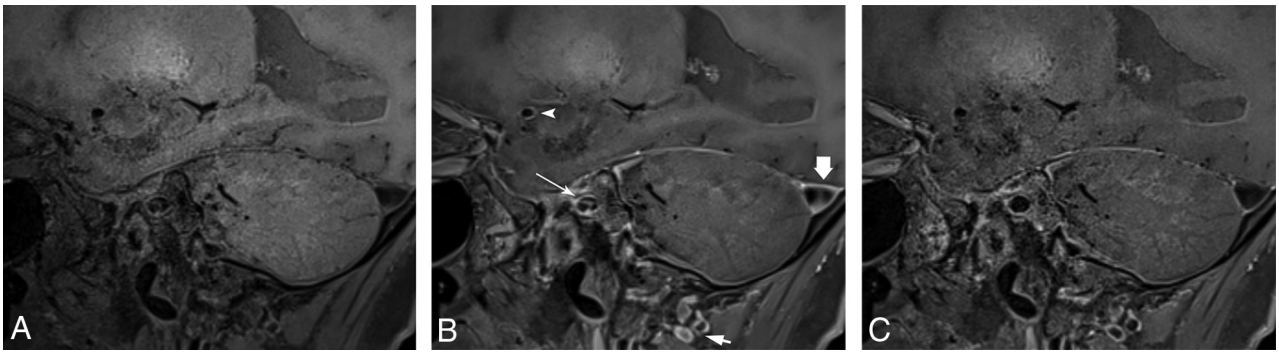

FIG 3. Sagittal T1-SPACE precontrast (*A*) shows a normal right M1 MCA segment without wall thickening. Sagittal T1-SPACE postcontrast (*B*) shows eccentric wall enhancement along the posterior, superior, and inferior walls of the M1 MCA (*arrowhead*) and the right V4 vertebral artery (*short arrow*) as well as nonsuppression of luminal signal in the right petrous ICA (*long arrow*) and the transverse sinus (*thick arrow*). Sagittal T1-DANTE-SPACE (*C*) shows the normal wall appearance of the right M1 MCA and V4 vertebral artery segments, similar to precontrast acquisition, and suppression of the venous signal.

agreement was with motion (0.938). The quantitative metrics of the lumen and wall area had excellent interreader agreement (0.969 and 0.942, respectively). The readers had good agreement for the lumen and wall-to-lumen contrast ratio (0.809 and 0.765, respectively).

In total 114 (57 SPACE, 43 DANTE-CAIPI-SPACE, and 14 DANTE-SPACE) sequences achieved sufficient lesion-pattern grades (1 or 2) to be reviewed for lesion pattern, with substantial overall interreader agreement (κ = 0.734). By means of consensus assessments, SPACE and DANTE-CAIPI-SPACE showed excellent agreement for lesion pattern (κ = 0.906), while SPACE and DANTE-SPACE had moderate agreement (κ = 0.512); 50.9% and 48.2% of cases showed an eccentric pattern on T1-SPACE and T1-DANTE-CAIPI-SPACE/T1-DANTE-SPACE, respectively.

DISCUSSION

The current study compares quantitative and qualitative image-quality assessments of conventional postcontrast T1-SPACE with either T1-DANTE or T1-DANTE-CAIPI-SPACE IVW. T1-DANTE-CAIPI-SPACE showed significant improvement in image quality, arterial and venous blood suppression, lesion conspicuity, and reduced artifact severity and motion, however, with lower SNR scores and quantitative metrics of SNR compared with T1-SPACE. There was a reduction in the scan time of 37% with T1-DANTE-CAIPI-SPACE. T1-DANTE-SPACE showed significant improvements in all of the above qualitative assessments compared with T1-SPACE with the exception of motion, however, with 7% increased scan times. There were no significant quantitative metric differences between T1-SPACE and T1-DANTE-SPACE. Arterial nonsuppression artifacts on T1-SPACE most frequently affected the vertebral artery (75.3%) and petrous ICA (44.9%) segments, while venous artifacts most frequently affected the cortical veins (65.2%) and dural venous sinuses (36%). To our knowledge, no prior study has compared T1-SPACE with implementations of DANTE for blood suppression and CAIPI for imaging acceleration for IVW applications in a real-world clinical environment. These findings support the value of using DANTE for arterial and venous blood suppression in clinical IVW applications. The decision about whether to also use CAIPI for imaging acceleration depends on the clinical needs and workflow balanced against the need for higher SNR, which can be further impacted when using high-resolution imaging. While not appreciated in this evaluation, lower SNR as seen with DANTE-CAIPI may limit the image quality of IVW techniques. On the basis of the evaluations, however, the improved blood suppression and reduced motion artifacts with DANTE-CAIPI offset the SNR limitation in this study.

Table 4: SPACE versus DANTE-SPACE (average score of 2 reviewers)[a]

	SPACE	DANTE-SPACE	*P* Value
Qualitative measurements			
Image quality	2.5 (2–3)	2 (1.5–2.5)	<.001
SNR	2 (2–2.5)	2 (1.5–2.5)	<.001
Artifacts	3.5 (3–4)	2.5 (2–3)	<.001
Art. blood suppression	3 (2.625–3.5)	1.5 (1–1.875)	<.001
Lesion	2.5 (2–3)	1.75 (1–2)	<.001
Ven. blood suppression	3 (2–3)	2 (1.5–2)	<.001
Motion	0.5 (0–2.75)	0.75 (0–2)	.50
Quantitative measurement			
Lumen area (mm^2)	5.9 (4.5–8.4)	6.8 (4.9–8.4)	.66
Wall area (mm^2)	14.4 (9.9–18.2)	14.1 (10.9–20.1)	.09
Lumen CR	0.33 (0.26–0.55)	0.35 (0.26–0.53)	.22
Wall lumen CR	2.2 (1.8–2.4)	2.2 (1.9–2.6)	.46

Note:—Art. indicates arterial; Ven., venous; CR, contrast ratio.
[a] Values are expressed as median (interquartile range).

Optimal IVW requires a combination of sufficient SNR, high spatial resolution, and optimal blood suppression for vessel wall visualization and vasculopathy evaluation. Currently, T1WI fast spin-echo variable refocusing flip angle sequences are the most often used 3D IVW sequences.[3] These sequences use a varying flip angle sweep to maintain stable signal over the long echo-trains and have high intrinsic black-blood properties due to intravoxel dephasing among the fast-spinning protons.[21] 3D techniques, however, are susceptible to incomplete blood suppression, especially after intravenous gadolinium administration, which results in time-to-inversion shortening of blood.[22] The high-resolution requirements also result in reduced SNR, leading to increased background noise and luminal signal.[23] This is especially true in certain pathologies such as aneurysms, in which slow and turbulent flow within the aneurysm sac could be mistaken for aneurysm wall enhancement.[10] Apart from the technical requirements, longer acquisition sequence times hinder widespread clinical use, especially in critically ill, unstable, and noncooperative patients. Longer acquisition times often translate to increased patient anxiety and discomfort and the likelihood of motion-degraded images, limiting diagnostic quality.[20] Long IVW scan times also negatively impact imaging throughput and may not be feasible to use in busy clinical practices.

Parallel imaging is the most commonly used acceleration technique; however, it comes with a loss of SNR by a factor of the square root of the acceleration factor secondary to reduced signal averaging, and it also results in spatially varying noise amplification (g-factor).[24] In comparison, CAIPI acceleration modifies the appearance of aliasing artifacts during data acquisition, thereby reducing the g-factor for a certain coil geometry and a certain imaging protocol and has been shown to be superior to standard 2D generalized autocalibrating partially parallel acquisition in terms of signal loss and image quality, especially in the central imaging FOV.[19]

The DANTE preparation module strengthens the black-blood effect by a series of nonselective low flip-angle pulses interleaved with gradient pulses, resulting in a spoiling effect in which flowing spins cannot achieve a steady-state. In addition to providing robust arterial blood suppression, DANTE significantly improves venous blood suppression.[22] Our study showed similar improvements in arterial and venous blood suppression with DANTE implementation in a larger cohort and applied to the intracranial vasculature. Cho et al[7] compared 3D T1-SPACE and BrainView (Philips Healthcare) with and without DANTE or MSDE in 14 healthy volunteers and found no significant difference in image-quality assessments whether DANTE was included or not. Their study, however, focused only on mid-M1 and M2 and distal basilar artery segments, while we evaluated the full intracranial and visualized extracranial vasculature with qualitative assessment. The quantitative assessment in our study, similarly, did not show any significant difference between T1-SPACE and T1-DANTE-SPACE and lower contrast ratios on T1-DANTE-CAIPI-SPACE relative to T1-SPACE. Specific segments, however, were most commonly involved with arterial flow artifacts on qualitative assessment in our study, specifically the petrous ICA and vertebral arteries, segments not evaluated by Cho et al. However, arterial flow artifacts were seen in all segments. Kalsoum et al[10] evaluated 22 patients with 30 intracranial aneurysms with T1-SPACE and MSDE-T1-SPACE and found that 10/30 aneurysms showed wall enhancement on T1-SPACE compared with 2/30 on MSDE-T1-SPACE ($P < .001$) from artifactual enhancement on T1-SPACE secondary to flow artifacts, similar to findings in the current study. Our study, however, evaluated a different flow-suppression technique (DANTE), incorporated imaging acceleration with CAIPI, and evaluated various vasculopathies that present in a routine clinical work-up.

Our study has several limitations. First, while the sample size is sufficient for technique comparison, larger sample sizes would be needed for technique comparison for individual vasculopathies. Second, we evaluated only a limited number of blood-suppression and imaging-acceleration techniques. We did not include compressed sensing or artificial intelligence reconstruction approaches for imaging acceleration, nor did we include MSDE for blood suppression. Due to the impact on the SNR of MSDE, similar high resolution was difficult to achieve with IVW protocols for the current study. We also did not compare T1-DANTE-CAIPI-SPACE and T1-DANTE-SPACE head-to-head. These comparisons would be valuable to see in a future larger study. Future large-cohort studies are needed to validate our results and to further optimize imaging protocols. Third, while ratings were performed randomly and independently for each acquisition, an experienced rater would be able to differentiate techniques, potentially limiting absolute blinding to acquisition.

CONCLUSIONS

Accelerated and blood-suppressed post-contrast T1-DANTE-CAIPI-SPACE had fewer image artifacts, less motion, improved blood suppression and a shorter scan time, but lower qualitative and quantitative SNR ratings relative to conventional T1-SPACE IVW. Blood-suppressed post-contrast T1-DANTE-SPACE had superior SNR, blood suppression, higher image quality and fewer image artifacts, but slightly longer scan time relative to T1-SPACE.

Disclosure forms provided by the authors are available with the full text and PDF of this article at www.ajnr.org.

REFERENCES

1. de Havenon A, Yuan C, Tirschwell D, et al. **Nonstenotic culprit plaque: the utility of high-resolution vessel wall MRI of intracranial vessels after ischemic stroke.** *Case Rep Radiol* 2015;2015:356582 CrossRef Medline
2. Gariel F, Ben Hassen W, Boulouis G, et al. **Increased wall enhancement during follow-up as a predictor of subsequent aneurysmal growth.** *Stroke* 2020;51:1868–72 CrossRef Medline
3. Mandell DM, Mossa-Basha M, Qiao Y, et al; Vessel Wall Imaging Study Group of the American Society of Neuroradiology. **Intracranial vessel wall MRI: principles and expert consensus recommendations of the American Society of Neuroradiology.** *AJNR Am J Neuroradiol* 2017;38:218–29 CrossRef Medline
4. Mossa-Basha M, de Havenon A, Becker KJ, et al. **Added value of vessel wall magnetic resonance imaging in the differentiation of Moyamoya vasculopathies in a non-Asian cohort.** *Stroke* 2016;47:1782–88 CrossRef Medline
5. Mossa-Basha M, Shibata DK, Hallam DK, et al. **Added value of vessel wall magnetic resonance imaging for differentiation of nonocclusive intracranial vasculopathies.** *Stroke* 2017;48:3026–33 CrossRef Medline
6. Qiao Y, Anwar Z, Intrapiromkul J, et al. **Patterns and implications of intracranial arterial remodeling in stroke patients.** *Stroke* 2016;47:434–40 CrossRef Medline
7. Cho SJ, Jung SC, Suh CH, et al. **High-resolution magnetic resonance imaging of intracranial vessel walls: comparison of 3D T1-weighted turbo spin echo with or without DANTE or iMSDE.** *PLoS One* 2019;14:e0220603 CrossRef Medline
8. Dieleman N, Yang W, van der Kolk AG, et al. **Qualitative evaluation of a high-resolution 3D multi-sequence intracranial vessel wall protocol at 3 Tesla MRI.** *PLoS One* 2016;11:e0160781 CrossRef Medline
9. Hu Z, van der Kouwe A, Han F, et al. **Motion-compensated 3D turbo spin-echo for more robust MR intracranial vessel wall imaging.** *Magn Reson Med* 2021;86:637–47 CrossRef Medline
10. Kalsoum E, Chabernaud Negrier A, Tuilier T, et al. **Blood flow mimicking aneurysmal wall enhancement: a diagnostic pitfall of vessel wall MRI using the postcontrast 3D turbo spin-echo MR imaging sequence.** *AJNR Am J Neuroradiol* 2018;39:1065–67 CrossRef Medline
11. Mossa-Basha M, Huynh TJ, Hippe DS, et al. **Vessel wall MRI characteristics of endovascularly treated aneurysms: association with angiographic vasospasm.** *J Neurosurg* 2018;131:859–67 CrossRef Medline
12. Mossa-Basha M, Hwang WD, De Havenon A, et al. **Multicontrast high-resolution vessel wall magnetic resonance imaging and its value in differentiating intracranial vasculopathic processes.** *Stroke* 2015;46:1567–73 CrossRef Medline
13. Yang Q, Deng Z, Bi X, et al. **Whole-brain vessel wall MRI: Aa parameter tune-up solution to improve the scan efficiency of three-dimensional variable flip-angle turbo spin-echo.** *J Magn Reson Imaging* 2017;46:751–57 CrossRef Medline
14. Zhu C, Tian B, Chen L, et al. **Accelerated whole brain intracranial vessel wall imaging using black blood fast spin echo with compressed sensing (CS-SPACE).** *MAGMA* 2018;31:457–67 CrossRef Medline
15. Cornelissen BMW, Leemans EL, Coolen BF, et al. **Insufficient slow-flow suppression mimicking aneurysm wall enhancement in magnetic resonance vessel wall imaging: a phantom study.** *Neurosurg Focus* 2019;47:E19 CrossRef Medline
16. Wang J, Helle M, Zhou Z, et al. **Joint blood and cerebrospinal fluid suppression for intracranial vessel wall MRI.** *Magn Reson Med* 2016;75:831–38 CrossRef Medline
17. Zhu C, Graves MJ, Yuan J, et al. **Optimization of improved motion-sensitized driven-equilibrium (iMSDE) blood suppression for carotid artery wall imaging.** *J Cardiovasc Magn Reson* 2014;16:61 CrossRef
18. Balu N, Zhou Z, Hippe DS, et al. **Accelerated multi-contrast high isotropic resolution 3D intracranial vessel wall MRI using a tailored *k*-space undersampling and partially parallel reconstruction strategy.** *MAGMA* 2019;32:343–57 CrossRef Medline
19. Falkovskiy P, Brenner D, Feiweier T, et al. **Comparison of accelerated T1-weighted whole-brain structural-imaging protocols.** *Neuroimage* 2016;124:157–67 CrossRef Medline
20. Andre JB, Bresnahan BW, Mossa-Basha M, et al. **Toward quantifying the prevalence, severity, and cost associated with patient motion during clinical MR examinations.** *J Am Coll Radiol* 2015;12:689–95 CrossRef Medline
21. Qiao Y, Steinman DA, Qin Q, et al. **Intracranial arterial wall imaging using three-dimensional high isotropic resolution black blood MRI at 3.0 Tesla.** *J Magn Reson Imaging* 2011;34:22–30 CrossRef Medline
22. Xie Y, Yang Q, Xie G, et al. **Improved black-blood imaging using DANTE-SPACE for simultaneous carotid and intracranial vessel wall evaluation.** *Magn Reson Med* 2016;75:2286–94 CrossRef Medline
23. Kale SC, Chen XJ, Henkelman RM. **Trading off SNR and resolution in MR images.** *NMR Biomed* 2009;22:488–94 CrossRef Medline
24. Jara H, Yu BC, Caruthers SD, et al. **Voxel sensitivity function description of flow-induced signal loss in MR imaging: implications for black-blood MR angiography with turbo spin-echo sequences.** *Magn Reson Med* 1999;41:575–90 CrossRef Medline